Supporting Information for

Efficient PH_3 Removal over Cu-doped Active Carbon with Stable Active Cu^{2+} Species Enabled by Nitrogen Modification

Yihui He,[b] Lin Ye,[c] Wanglai Cen,[d] Jianjun Li,[ab] Dengrong Sun*[ab]

a College of Carbon Neutrality Future Technology, Sichuan University, Chengdu 610065, P. R. China

b College of Architecture and Environment, Sichuan University, Chengdu 610065, P. R. China

c College of Chemistry, Sichuan University, Chengdu 610065, P. R. China

d Institute of New Energy and Low Carbon Technology, Sichuan University, Chengdu, P. R. China

Corresponding Email: dengrongsun@hotmail.com (D. Sun), dengrongsun@scu.edu.cn (D. Sun)

Appendix S1: Characterization methods

The X-ray diffraction (XRD) patterns were acquired on a Malvern Panalytical X'Pert^3 Powder from 5-90° at 0.17°·s^{-1} and phases identified using MDI Jade 6.5 vs. JCPDS. The specific surface areas were measured using an N_2 adsorption analyzer (Micromeritics ASAP 2460) at 77 K and were calculated using a Brunauer-Emmett-Teller (BET) model. Before the analysis, all samples were degassed at 473 K for 3 h. The BET surface area, pore volume were calculated using desorption isotherms. The pore size distributions were obtained using the BJH method. The scanning electron microscope (SEM, Tescan MIRA LMS) equipped with the EDS system was used to observe the surface morphology and microstructure of the samples. The morphology and structure of the materials were characterized by a transmission electron microscope (TEM, JEOL-JEM 2100F) equipped with the EDS system (Oxford X-Max 80T) . The hydrogen temperature-programmed reduction (H_2-TPR) experiments were performed to test the reduction performance of the samples (VDsorb-91i) under the conditions of 10 vol% H_2 atmospheres and 10°C•min^{-1}. The basicity and alkaline site number of the adsorbents were determined using CO_2-TPD with an VDsorb-91i instrument under the conditions of 10 vol% He atmospheres, and 10°C•min^{-1}, and detected the desorbed gas with TCD. The Fourier transform infrared spectroscopy (FT-IR) analysis was carried out using an infrared spectrophotometer (Shimadzu IRTracer-100). The instrument was scanned 32 times over a test range of 400-4000 cm $^{-1}$, and the resolution of the instrument was 4 cm $^{-1}$. The X-ray Photoelectron Spectroscopy (XPS) was performed on a Thermo Scientific Nexsa, processed with Avantage, with C1s at 284.5 eV as the standard. The concentration of PO_4^{3-} in the Cu-N-AC-D was measured with a Thermo Scientific Dionex Aquion ion chromatograph (IC), and the content of Cu was determined using an Agilent-5110 inductively coupled plasma optical emission spectrometer (ICP-OES).

Supplementary Figures

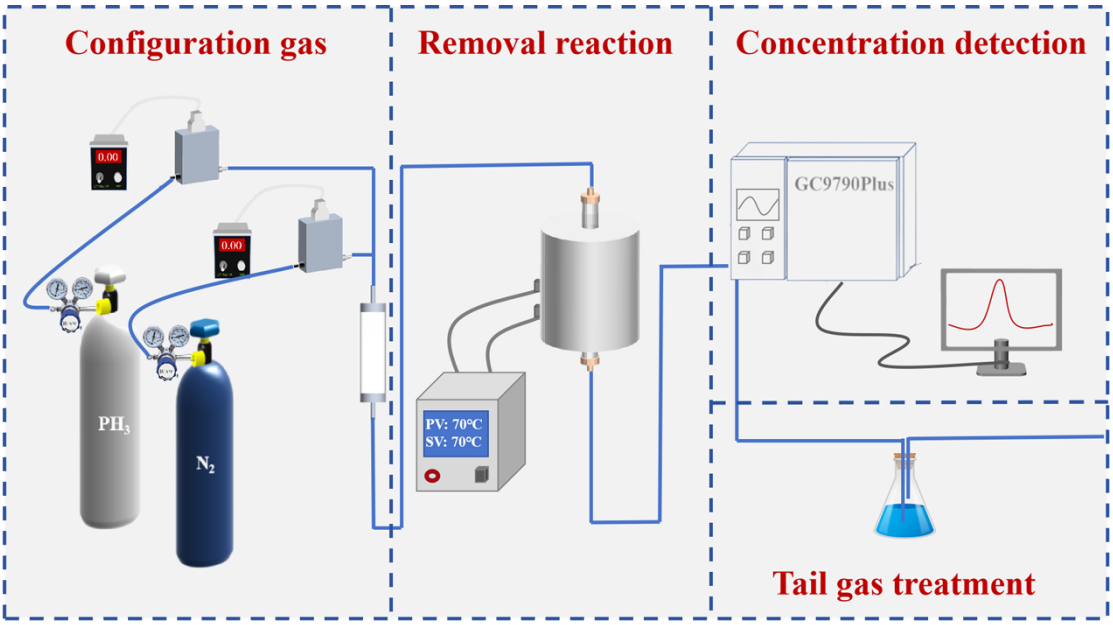

Figure S1. The reaction system for PH_3 purification.

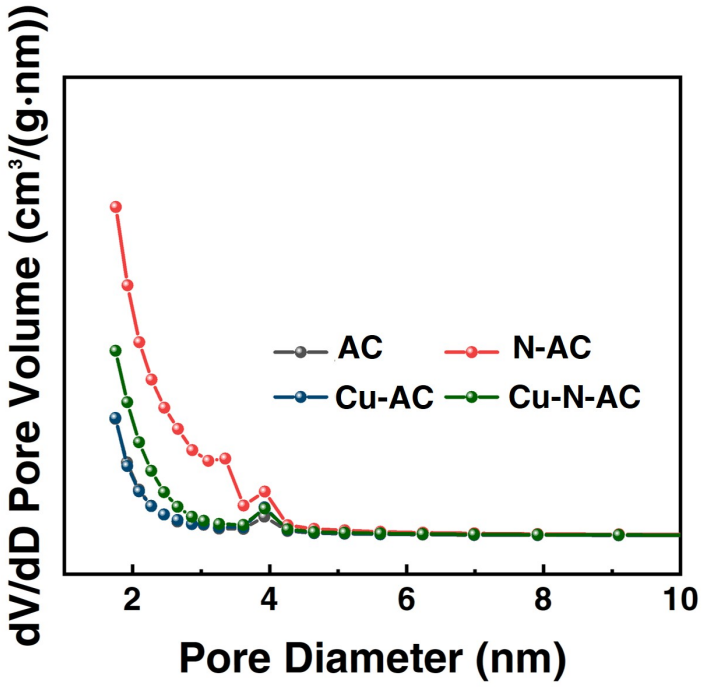

Figure S2. The pore size distributions of various samples.

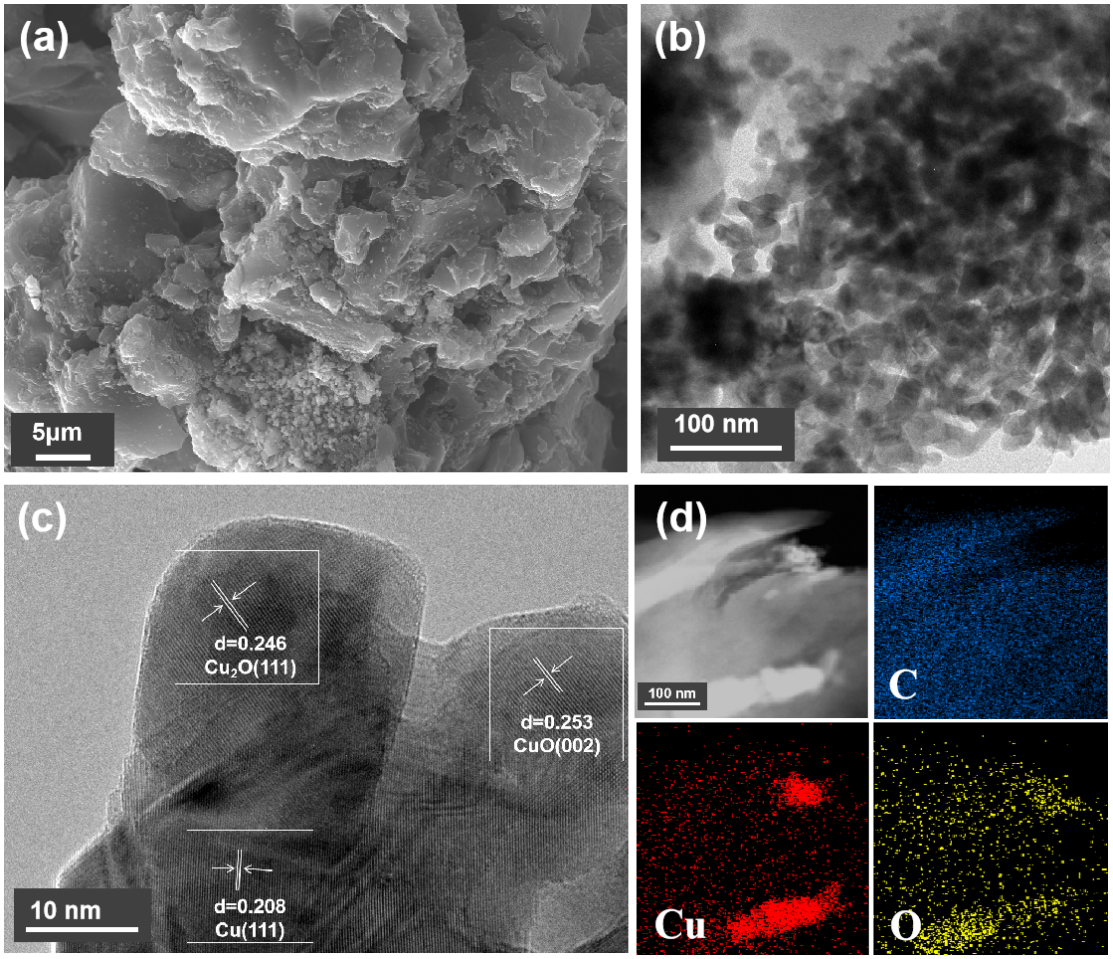

Figure S3. (a) SEM micrograph, (b) TEM micrograph, (c) HR-TEM image and (d) TEM-EDS mapping images of Cu-AC.

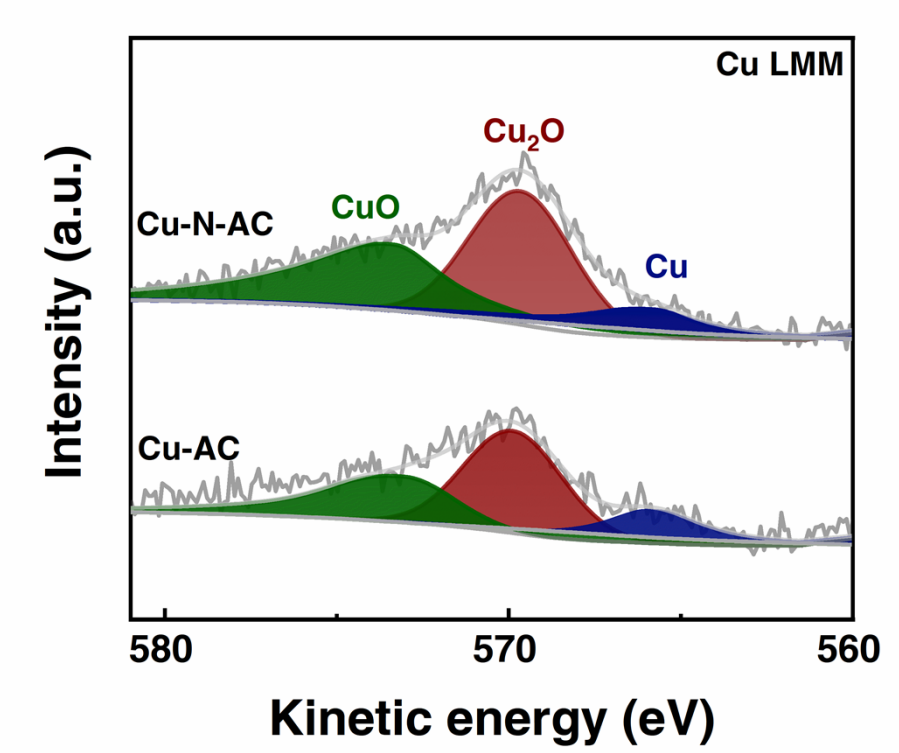

Figure S4. The Cu LMM spectra of Cu-AC and Cu-N-A

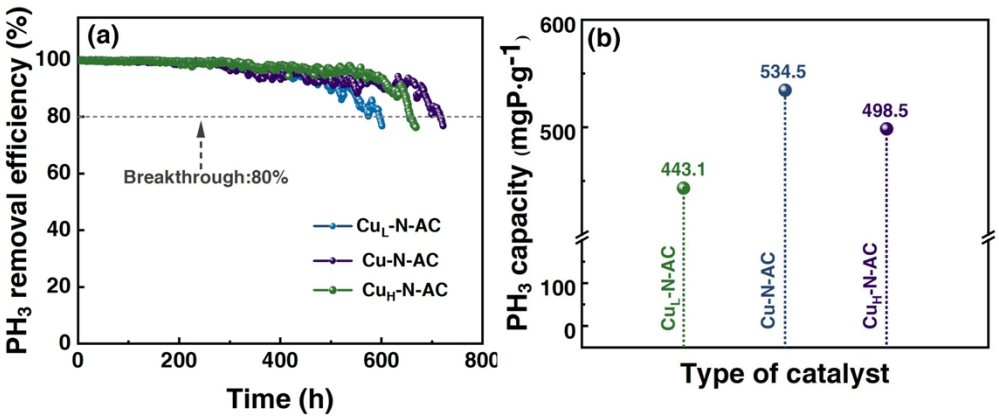

Figure S5. PH_3 removal performance over catalysts with different copper content. Cu_L-N-AC and Cu_H-N-AC are samples with lower and higher Cu loading amount as compared with Cu-N-AC. Cu_L-N-AC, Cu-N-AC and Cu_H-N-AC are prepared by dispersing N-AC in the solution of $Cu(NO_3)_2 \cdot 3H_2O$ with different concentrations of 0.05g/mL, 0.10g/mL and 0.15g/mL respectively.

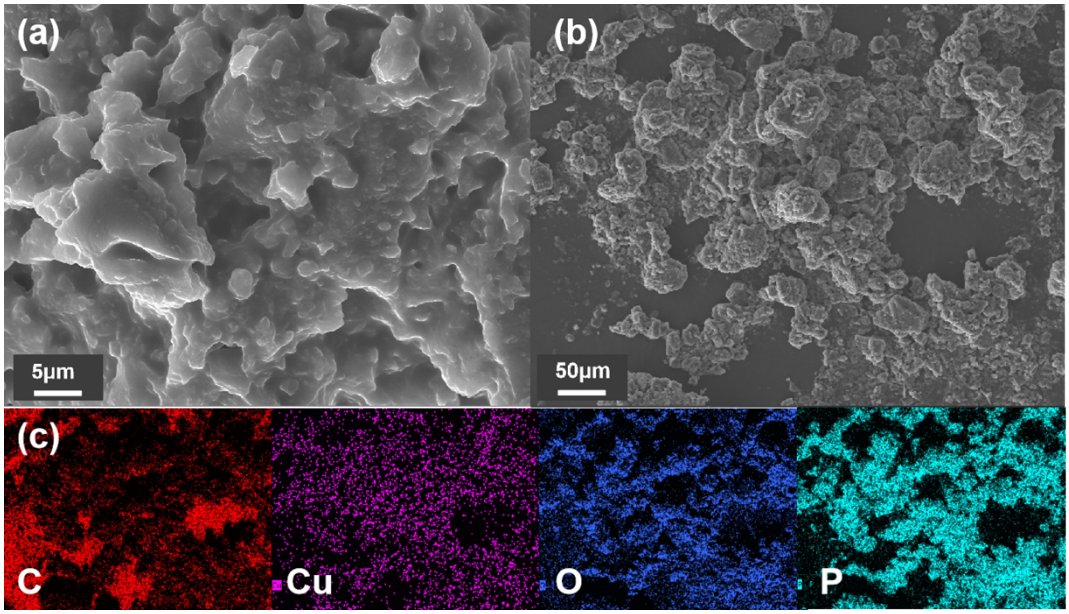

Figure S6. (a-b) SEM micrograph and (c) SEM-EDS mapping images of Cu-N-AC-D.

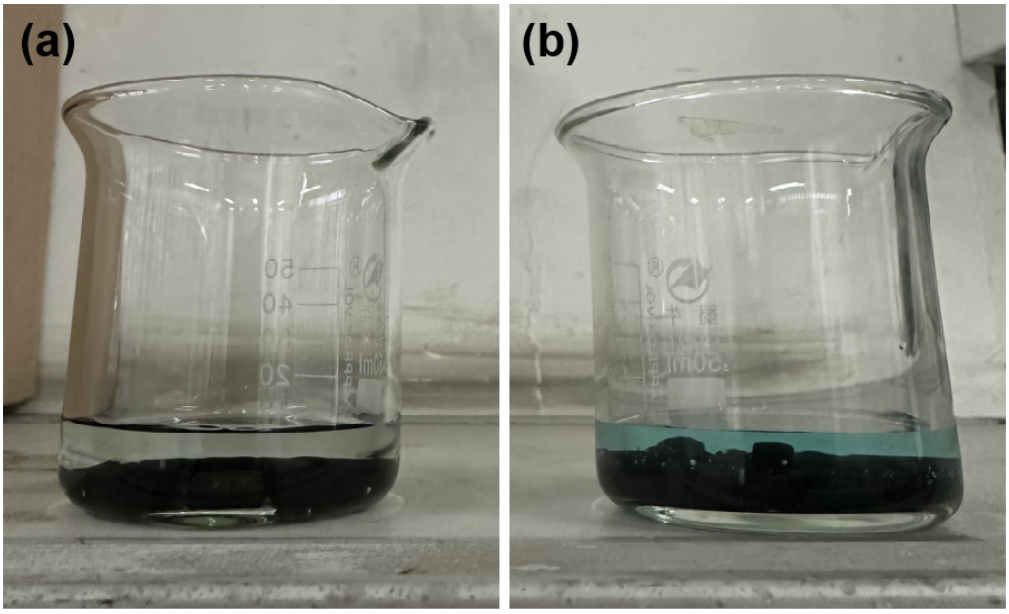

Figure S7. (a) Cu-N-AC-D immersed in water and (b) Cu-AC-D immersed in water.

Supplementary Tables

Table S1. The surface area and pore size distribution of different samples.

Sample	S ($m^2 \cdot g^{-1}$)	V_{total} ($cm^3 \cdot g^{-1}$)
AC	953.8	0.43
N-AC	1081.8	0.54
Cu-AC	850.2	0.37
Cu-N-AC	824.7	0.38

S: specific surface area; V_{total}: total pore volume;

Table S2. Proportion of copper species in samples determined from XPS spectra.

Sample	Copper Species	Binding energy (eV)	Atomic ratio (%)*
Cu-AC	Cu	932.1	31.5
	Cu_2O	933.5	40.9
	CuO	935.1	27.6
Cu-N-AC	Cu	--	--
	Cu_2O	933.7	30.9
	CuO	935.4	69.1
Cu-N-AC-D	Cu	933.7	36.9
	Cu_2O	934.4	27.8
	CuO	935.7	35.3
Cu-N-AC-R	Cu	933.2	9.7
	Cu_2O	933.8	38.4
	CuO	935.7	51.9

*Atomic ratio of different copper species obtained from the XPS results.

Table S3. Proportion of nitrogen species in Cu-AC and Cu-N-AC determined from XPS spectra.

Sample	Nitrogen Species	Binding energy (eV)	Atomic ratio (%)*
N-AC	pyridinic-N	399.6	44.6
	pyrrolic-N	401.4	30.2
	N-Oxides	407.1	25.2
Cu-N-AC	pyridinic-N	397.8	24.0
	pyrrolic-N	401.3	38.4
	N-Oxides	406.5	37.6

*Atomic ratio of different nitrogen species obtained from the XPS results.

Table S4. Proportion of oxygen species in different samples determined from XPS spectra.

Sample	Oxygen Species	Atomic ratio (%)*
Cu-AC	O_{α}	17.3
	O_{β}	56.2
	O_{γ}	26.5
Cu-N-AC	O_{α}	22.8
	O_{β}	44.6
	O_{γ}	32.6
Cu-N-AC-D	O_{α}	9.9
	O_{β}	30.5
	O_{γ}	59.6

*Atomic ratio of different Oxygen Species obtained from the XPS results.

Table S5. Summary of PH_3 removal performance of previously reported materials.

Adsorbents	Gas Composition	Temperature (◦ C)	Breakthrough Standard	Breakthrough Capacity (mg • g^{-1})	Ref
30Cu@TiO_2	N_2 + 1000 ppm PH_3; 30000h^{-1}	120 ℃	100 ppm (10%)	135.73	1
CuO/AC	N_2 + 231 ppm PH_3 + 1.6% O_2; 750 h^{-1}	110 ℃	3.3 ppm (1.4%)	96.08	2
Cu/ACF-NH_3	N_2 + 400 ppm H_2S + 600 ppm PH_3 + 1% O_2. 2000 mL/(g • hr)	90 ℃	240ppm (40%)	121.6	3
$Cu_{0.15}$/ACF	N_2 + 300 ppm H_2S+ 600ppm PH_3 + 0.5% O_2; 10000 h^{-1}	90 ℃	600ppm (100%)	132.1	4
CuO-ZnO-La_2O_3/AC	N_2 + 874 ppm PH_3 + 1% O_2; 5000 h^{-1}	70 ℃	87.4ppm (10%)	147.11	5
Cu_{30}/TiO_2	N_2 + 1000 ppm PH_3 + 1% O_2; 60000mL • h^{-1} • g^{-1}	90 ℃	30ppm (3%)	136.2	6
UG@Cu-2	N_2 + 1000 ppm PH_3; 30000 h^{-1}	60 ℃	30ppm (3%)	318.58	7
$Ce_1Cu_{30}O_X$/ HZSM-5	N_2 + 800 ppm PH_3+ 1% O_2; 15000 mL • h^{-1} • g^{-1}	90 ℃	320 ppm (40%)	114.36	8
Cu_{45}-Fe_8/SBA-15	N_2 + 200 ppm H_2S+ 800ppm PH_3 + 0.5% O_2; 10000 h^{-1}	80 ℃	320 ppm (40%)	120.05	9
Cu/HZSM-5-[S1]	N_2 + 450 ppm H_2S+ 600ppm PH_3 + 1% O_2; 20000 mL • cm^{-3} • h^{-1}	90 ℃	240 ppm (40%)	150.9	10
Cu-N-AC	N_2 +140 ppm PH_3; 4000 mL·h^{-1}·g^{-1}	70 ℃	28ppm (20%)	534.5	This work

Table S6. The content of copper in different samples determined from ICP-OES.

Sample	Copper Content (mg/g)	Copper Content (%)
Cu-AC	38.4	3.84
Cu-N-AC	31.8	3.18

Reference

1 J. Feng, K. Li, X. Wang, X. Yang, K. Hu, F. Wang, P. Ning, L. Jia and J. Cai, Two Birds with One Stone: Copper-Based Adsorbents Used for Photocatalytic Oxidation of Hg^0 (Gas) after Removal of PH_3, *Environ. Sci. Technol.*, 2023, **57**, 4632–4642.

2 J. Feng, F. Wang, C. Wang, K. Li, P. Ning, X. Sun and L. Jia, Ce-doping CuO/HZSM-5 as a regenerable sorbent for Adsorption–Oxidation removal of PH_3 at low temperature, *Sep. Purif. Technol.*, 2021, **277**, 119420.

3 J. Feng, F. Wang, C. Wang, K. Li, X. Sun and P. Ning, Cu/HZSM-5 Sorbent Treated by NH_3 Plasma for Low-Temperature Simultaneous Adsorption-Oxidation of H_2S and PH_3, *ACS Appl. Mater. Interfaces*, 2021, **13**, 24670–24681.

4 L. Jia, X. Yang, K. Hu, J. Feng, F. Wang, K. Li, X. Sun, F. Wang and P. Ning, Preparation of $XCu@TiO_2$ adsorbent for high-efficient PH_3 removal in anaerobic environment and evaluation of desulfurization activity of deactivated adsorbent, *Chem. Eng. J.*, 2023, **457**, 141277.

5 Z. Ren, S. Quan, Y. Zhu, L. Chen, W. Deng and B. Zhang, Purification of yellow phosphorus tail gas for the removal of PH_3 on the spot with flower-shaped CuO/AC, *RSC Adv.*, 2015, **5**, 29734–29740.

6 X. Song, S. Li, K. Li, P. Ning, C. Wang, X. Sun and Y. Wang, Preparation of Cu-Fe composite metal oxide loaded SBA-15 and its capacity for simultaneous catalytic oxidation of hydrogen sulfide and phosphine, *Micropor. and Mesopor. Mater.*, 2018, **259**, 89–98.

7 Y. Tang, J. Feng, P. Ning, F. Wang, X. Sun and K. Li, Low-Temperature Efficient Removal of PH_3 over Novel Cu-Based Adsorbent in an Anaerobic Environment, *Chem. Eng. J.*, 2023, **461**, 142078.

8 Y. Wang, P. Ning, R. Zhao, K. Li, C. Wang, X. Sun, X. Song and Q. Lin, A Cu-modified active carbon fiber significantly promoted H_2S and PH_3 simultaneous removal at a low reaction temperature, *Front. Environ. Sci. Eng.*, 2021, **15**, 132.

9 X. Yang, K. Li, C. Wang, F. Wang, X. Sun, Y. Ma, Y. Li, L. Shi and P. Ning, Cu/ACF adsorbent modified by non-thermal plasma for simultaneous adsorption–oxidation of H_2S and PH_3, *J. Environ. Sci.*, 2023, **127**, 641–651.

10 H. Yi, Q. Yu, X. Tang, P. Ning, L. Yang, Z. Ye and J. Song, Phosphine Adsorption Removal from Yellow Phosphorus Tail Gas over $CuO{-}ZnO{-}La_2O_3$/Activated Carbon, *Ind. Eng. Chem. Res.*, 2011, **50**, 3960–3965.